

This article was downloaded by: [Central Electrochemical Res Inst]

On: 02 February 2012, At: 01:52

Publisher: Taylor & Francis

Informa Ltd Registered in England and Wales Registered Number: 1072954 Registered office: Mortimer House, 37-41 Mortimer Street, London W1T 3JH, UK



## Environmental Technology

Publication details, including instructions for authors and subscription information:

<http://www.tandfonline.com/loi/tent20>

### Thin wetted film cylindrical flow photo reactor for the degradation of Procion blue H-B dye over $\text{TiO}_2$ and $\text{ZnO}$

M.G. Neelavannan<sup>a</sup> & C. Ahmed Basha<sup>a</sup>

<sup>a</sup> Pollution Control Section, Central Electrochemical Research Institute, Karaikudi, India

Available online: 17 Jun 2011

To cite this article: M.G. Neelavannan & C. Ahmed Basha (2011): Thin wetted film cylindrical flow photo reactor for the degradation of Procion blue H-B dye over  $\text{TiO}_2$  and  $\text{ZnO}$ , Environmental Technology, 32:8, 825-835

To link to this article: <http://dx.doi.org/10.1080/09593330.2010.514948>

PLEASE SCROLL DOWN FOR ARTICLE

Full terms and conditions of use: <http://www.tandfonline.com/page/terms-and-conditions>

This article may be used for research, teaching, and private study purposes. Any substantial or systematic reproduction, redistribution, reselling, loan, sub-licensing, systematic supply, or distribution in any form to anyone is expressly forbidden.

The publisher does not give any warranty express or implied or make any representation that the contents will be complete or accurate or up to date. The accuracy of any instructions, formulae, and drug doses should be independently verified with primary sources. The publisher shall not be liable for any loss, actions, claims, proceedings, demand, or costs or damages whatsoever or howsoever caused arising directly or indirectly in connection with or arising out of the use of this material.

## Thin wetted film cylindrical flow photo reactor for the degradation of Procion blue H-B dye over TiO<sub>2</sub> and ZnO

M.G. Neelavannan\* and C. Ahmed Basha

*Pollution Control Section, Central Electrochemical Research Institute, Karaikudi, India*

*(Received 15 July 2009; Accepted 9 August 2010)*

A thin wetted film cylindrical flow reactor was fabricated for photocatalytic oxidation of Procion blue H-B dye in textile washwater with the suspensions of TiO<sub>2</sub> and ZnO. The disappearance of colour and organic reduction were studied in terms of the removal of colour and chemical oxygen demand (COD). Operating parameters such as effect of pH, UV irradiation with and without catalyst, initial concentration of dye and effect of flow rate were studied and kinetics of Procion blue H-B dye has been studied over TiO<sub>2</sub> and ZnO surfaces. Since adsorption is the prerequisite condition for decolorization / degradation of dye molecules in the presence of heterogeneous catalysis, the Langmuir and Freundlich isotherms were examined to verify the adsorption intensity. The results clearly demonstrated that, the optimum loading of the photocatalyst was found to be 300 and 400 mg/L of TiO<sub>2</sub> and ZnO, respectively. The maximum COD reduction efficiency was 68% for TiO<sub>2</sub> and 58% for ZnO. On the other hand, the colour removal efficiency was found to be 74% and 69%, respectively for TiO<sub>2</sub>- and ZnO-assisted systems under optimum conditions. Conclusively, these two semiconductors could degrade Procion blue H-B dye at different time intervals and both isotherms fit well.

**Keywords:** Procion blue H-B dye; photo catalysis; TiO<sub>2</sub>; ZnO; washwater; COD

### 1. Introduction

Reactive dyes are some of the most commonly used dyes in the textile industry. They are coloured compounds, which have a high solubility in water and have reactive groups. The stability and resistance of dyes to degradation have made colour removal from textile wastewater difficult by conventional biological treatment plants [1] and considerable research is focused on addressing this problem [2,3,4]. Conventionally effluents containing organics are treated with adsorption, biological oxidation, coagulation, etc. Though the conventional methods have individual advantages, they lack effectiveness if applied individually. For example, biological treatment is the most efficient and economic way of reducing the environmental impact of the industrial effluents containing organic pollutants, but this technique is time consuming and cannot be employed for textile effluent, as textile effluent is recalcitrant to biodegradation. On the other hand, the physical adsorption is expensive and difficult for adsorbent regeneration. Further, biological and chemical methods generate a considerable quantity of sludge, which itself requires treatment. Due to the large variability of the composition of textile wastewater, most of the traditional methods are becoming inadequate [5,6,7].

Numerous biodegradability studies on dyes have shown that reactive dyes are not likely to be biodegradable under aerobic conditions [8,9,10]. Due to the stability of modern dyes, conventional biological treatment methods for industrial wastewater are ineffective, frequently resulting in an intensely coloured discharge from the treatment facilities. Additionally, they are readily reduced under anaerobic conditions to potentially hazardous aromatic amines. Thus, there is a need for developing treatment methods that are more effective in eliminating dyes from a waste stream at its source [11,12].

New technologies of wastewater purification leading to the complete mineralization of organic pollutants are now considered as the most suitable solution. The degradation of many organic compounds by semiconductor particles, such as TiO<sub>2</sub>, ZnO, ZrO<sub>2</sub>, WO<sub>3</sub>, SrO<sub>2</sub>, Fe<sub>2</sub>O<sub>3</sub>, CeO<sub>2</sub>, CdS and ZnS have been attempted for the photocatalytic degradation of a wide variety of environmental contaminants. But TiO<sub>2</sub> and ZnO have been widely recognized as a promising method for the treatment of water and wastewater [13–18]. The efficiency of photocatalytic processes seems to depend on several different characteristics of the semiconductor particles, such as their surface properties, the position of their

\*Corresponding author. Email: mgneelus@cecri.res.in

band gap potentials, and the mobility and recombination rate of the charge carriers generated by UV-light absorption. Moreover, a relevant role is also played by the chemical and adsorption properties of the degradation substrate, depending also on experimental conditions, such as pH and the substrate to photocatalyst concentration ratio.

Even though many catalysts have been attempted for the photocatalytic degradation of organic pollutants, only a handful of studies have been carried out which compare the efficiency of different catalysts for a particular organic compound under identical experimental conditions. Hence, attempts have been made to study the activity of two photo catalysts namely  $\text{TiO}_2$  (Ranbaxy) and  $\text{ZnO}$  in the photocatalytic degradation of Procion blue H-B dye.

It is generally accepted that the photocatalytic reaction is initiated by band gap photo excitation of the titanium dioxide on zinc oxide with UV light having energy equal to or larger than the band gap of the semiconductor (3.2 eV). Electrons are photo excited to the conduction band from the valence band, producing electron-hole pairs within the semiconductor solid. Some of the electrons and holes migrate to the semiconductor and initiate redox reactions with adsorbates through interfacial electron transfer [19].

The main objective of this study was the fabrication of a novel, thin wetted film cylindrical flow photo reactor and the maximum removal of the Procion blue H-B dye in the textile wastewater by photocatalytic degradation. The photocatalytic degradation was investigated in the presence of titanium dioxide and of zinc oxide under different experimental conditions. In particular, the effect of pH, flow rate, UV irradiation with and without catalyst, initial concentration of dye, and sorption isotherms such as Langmuir and Freundlich were investigated on the removal of colour and reduction of COD.

## 2. Materials and methods

### 2.1. Materials

Textile wastewater which contains procion blue H-B dye was obtained from Tube knit Fashion Ltd, Tirupur. Initial concentration of wastewater was varied by the addition of distilled water. Initial pH of the wastewater was adjusted by adding HCl. Anatase  $\text{TiO}_2$  powder (98%) was purchased from Ranbaxy Laboratories, India and  $\text{ZnO}$  was purchased from Pure Drugs India.

### 2.2. Thin film photo reactor

The fabrication of a photocatalytic reactor with high efficiency for UV application was one of the objectives of the present study. The thin film photo reactor comprises a titanium cylindrical container (reactor) of

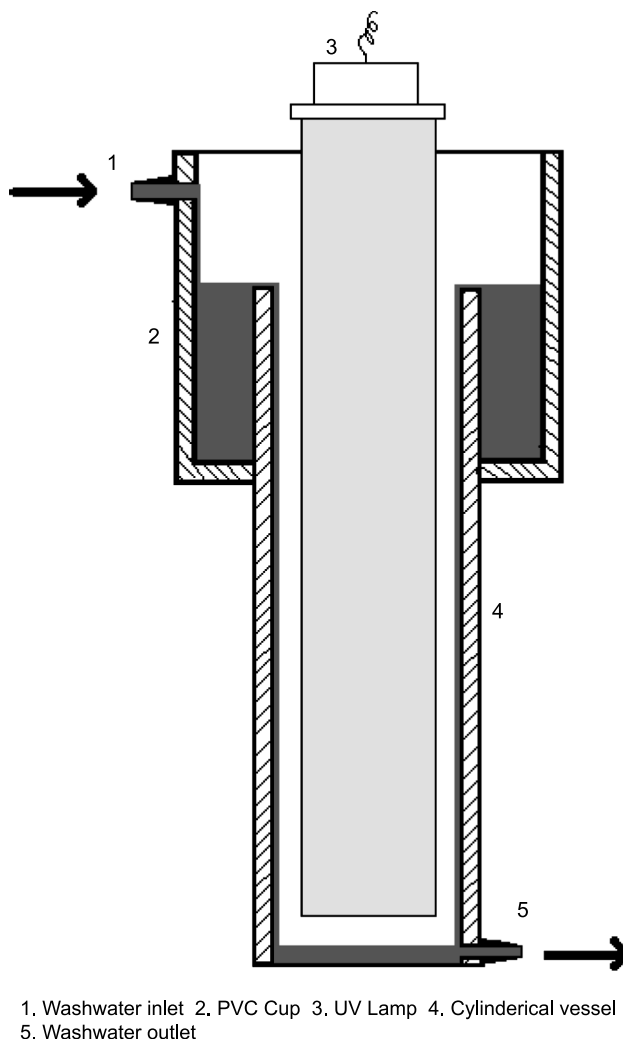
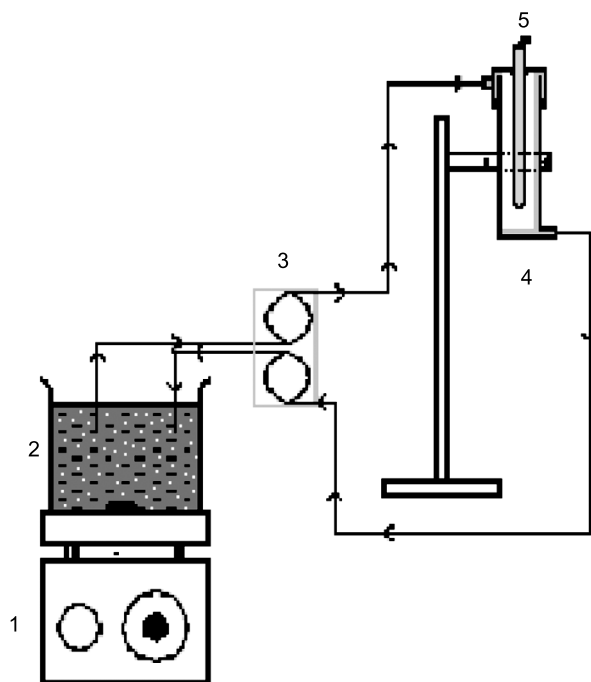


Figure 1. Cross-section view of thin film photo reactor.

diameter 50 mm and height of 270 mm. In order to store and allow the effluent along inside walls of the reactor as thin film a PVC cup was fixed on the top of the container. A pencil type 6 W medium pressure, mercury vapour immersion lamp of 25 mm diameter and of 270 mm height with a maximum emission at 365 nm was employed as a source for UV irradiation and it was fixed vertically in the centre of the cylindrical reactor with the help of PVC clamps. Provisions were also made for wastewater entry and exit in the photo reactor. The cross-section view of the thin film photo reactor is shown in Figure 1.

### 2.3. Methods

Textile wastewater was taken in the 1 litre beaker and placed on a magnetic stirrer. The magnetic stirrer was used to mix the photo catalysts and bring the molecules closer. In this work wastewater was affected by a batch



1. Magnetic Stirrer 2. Washwater 3. Peristaltic Pump.  
4. Thinfilm photo reactor. 5. UV lamp

Figure 2. Schematic diagram of experimental set up.

recirculation system. Washwater was sent to the PVC cup on the top of the photo reactor with the help of a double head peristaltic pump. The washwater from the reservoir was passed at the required flow rate to the photo reactor by adjusting the speed of peristaltic pump. After filling up the PVC cup, the effluent flows down as a thin wetted film on the wall of the photo reactor. The thin film of washwater was irradiated by a pencil type UV lamp. The treated washwater was sent back to the reservoir by using the second head of the peristaltic pump for recirculation. The schematic diagram of the experimental set up is shown in Figure 2. Washwater which was collected from industry was diluted using distilled water to get different concentrations. pH of the washwater was varied by adding hydrochloric acid.

#### 2.4. Analysis of COD

The chemical oxygen demand (COD) analysis was used to measure the amount of organic pollutants present in washwater indirectly. The basis for the COD analysis was that nearly all organic compounds can be fully oxidized to carbon dioxide with a strong oxidizing agent under acidic conditions. In this analysis, Potassium dichromate was used as a strong oxidizing agent under acidic conditions. 0.4 g of  $\text{HgSO}_4$  was placed in a reflux flask and an aliquot of the sample was added. This

sample was mixed well and 2 ml of 0.25N  $\text{K}_2\text{Cr}_2\text{O}_7$  solution was added. Then 3 ml of  $\text{H}_2\text{SO}_4 - \text{AgSO}_4$  reagent was slowly added while continuously swirling the flask. A condenser was connected in the flask and kept in the COD digester. This mixture was refluxed for at least 2 hours at about  $148^\circ\text{C}$ . The digested mixture was cooled and washed down the condenser with distilled water such that the washings fell into the flask. The unreacted  $\text{K}_2\text{Cr}_2\text{O}_7$  was titrated with the N/10 ferrous ammonium sulphate solution using ferroin as an indicator. The colour change at the end point was from blue green to wine red. A blank experiment with distilled water instead of the sample was also performed. The following formula was used to calculate COD:

$$\text{COD} = \frac{8000(b-s)n}{\text{volume of sample}} \times \text{dilution factor}$$

where  $b$  is the volume of FAS used in the blank sample,  $s$  is the volume of FAS in the original sample, and  $n$  is the normality of FAS.

#### 2.5. Analysis of colour removal

Choice of wavelength was selected by measuring the absorbance value of the sample at all wavelengths available in the NOVA 60 instrument. A wavelength which gives the maximum absorbance value was considered as a suitable wavelength (605 nm) for the Procion blue H-B dye. Samples were collected at an interval and measured the hourly absorbance values directly using the NOVA 60 (MERK) instrument at 605 nm. Percentage of colour removal can be calculated by the following formula:

$$\frac{\text{Initial absorbance} - \text{final absorbance}}{\text{Initial absorbance}} \times 100$$

#### 2.6. Kinetic studies

When photo catalyst is irradiated with UV, an electron is excited from the valence band (VB) to the conduction band (CB) leaving the hole behind in the VB. This is a rapid process occurring in femtoseconds [20]. In order to investigate the mechanism of sorption and potential rate controlling steps such as mass transport and chemical reaction processes, kinetic models have been used to test experimental data.

##### 2.6.1. The pseudo-first-order equation

The rate constant of adsorption can also be determined from the pseudo-first-order kinetic model given by Namasivayam and Ranganathan [21]. The differential equation is given as,

$$\frac{dq_t}{dt} = k_1(q_e - q_t) \quad (1)$$

where  $q_e$  and  $q_t$  are the amount of dye adsorbed (mg/g) on the adsorbent at the equilibrium and at time  $t$ , respectively and  $k_1$  is the rate constant of pseudo-first-order adsorption (L/min).

Integrating Equation (1) for the boundary conditions  $t=0$  to  $t=t$  and  $q=0$  to  $q_t$ , gives,

$$\log \left[ \frac{q_e}{q_e - q_t} \right] = \frac{k_1}{2.303} t \quad (2)$$

This is the integrated rate law for a pseudo-first-order reaction. Equation (2) can be rearranged to obtain a linear form:

$$\log \left[ 1 - \frac{q_t}{q_e} \right] = -\log \left[ \frac{k_1}{2.303} \right] t \quad (3)$$

In order to obtain the rate constant  $k_1$  and correlation coefficient  $R_1^2$  from the linear plots of  $\log \left( 1 - \frac{q_t}{q_e} \right)$  against  $t$  for different initial dye concentrations and sorbent dosages have been analysed.

### 2.6.2. The second-order equation

The second-order kinetic model equation is also based on the sorption capacity of the solid phase [22]. Contrary to the other model it predicts the behaviour over the whole time adsorption and is in agreement with an adsorption mechanism being the rate controlling step. If the rate of sorption is a second-order mechanism, the second-order chemisorptions kinetic rate equation is expressed as:

$$\frac{dq_t}{dt} = k_2(q_e - q_t)^2 \quad (4)$$

where  $q_e$  and  $q_t$  are the amount of dye adsorbed (mg/g) on the adsorbent at the equilibrium and at time  $t$ , respectively and  $k_2$  is the rate constant of second order. Integrating Equation (4) for the boundary conditions  $t=0$  to  $q_t$  gives:

$$\frac{1}{(q_e - q_t)} = \frac{1}{q_e} + k_2 t \quad (5)$$

This is known as the second-order equation. Equation (5) can be rearranged to obtain a linear form:

$$\frac{t}{q_t} = \frac{1}{k_2 q_e^2} + \frac{1}{q_e} t \quad (6)$$

The linear plots of  $t/q_t$  against  $t$  have been treated to obtain the rate constant  $k_2$  (g/mg min) for different initial dye concentrations and sorbent dosages. The initial adsorption rate ( $k_2 q_e^2$ ), and the correlation coefficients  $R_2^2$  were obtained from these plots.

### 2.6.3. The intra-particle diffusion equation

In any adsorption process, the rate limiting step has an important role that is known as the adsorption mechanism. Generally in a solid-liquid sorption process, the solute transfer is usually characterized by external mass transfer or intraparticle diffusion. There are three pathways to analyse the adsorption mechanism. The first path is known as film diffusion which is on the exterior surface, that the transfer of solute from bulk solution through the liquid film takes place. The second path is the particle diffusion where the transportation of the adsorbate within the pores of the adsorbent occurs and the third path is the adsorption of the adsorbate on the interior surface of the adsorbent. According to Weber and Morris [23], the rate constant for intraparticle diffusion is given by Equation (7):

$$q_t = k_{id} t^{1/2} \quad (7)$$

where  $q_t$  is the amount of dye adsorbed (mg/g) at time,  $t$  and  $K_{id}$  were calculated from the slope of  $q_t$  versus  $t^{1/2}$  for all initial dye concentrations and sorbent dosages have been analysed.

### 2.7. Mechanism of adsorption isotherms

Adsorption isotherms are important for the description of the interaction of molecules or ions of adsorbate with adsorbent surface sites and also, are critical in optimizing the use of adsorbent. Hence, the correlation of equilibrium data using either a theoretical or empirical equation is essential for the adsorption interpretation and prediction of the extent of adsorption. In the present study, Langmuir and Freundlich isotherm equations have been tested. Langmuir adsorption isotherm is based on the assumption that all adsorption sites are equivalent and adsorption in active sites is independent of whether the adjacent sites are occupied or not. Langmuir isotherm is often used to describe sorption of solutes from liquid solutions and is expressed by the following equation:



$$q_e = \frac{Q^0 b C_e}{1 + b C_e} \quad (8)$$

where  $C_e$  is the concentration of dye at equilibrium (mg/L),  $Q^0$  and  $b$  are Langmuir constants related to adsorption capacity and energy of adsorption respectively. The linear form of (8) is given by the following form:

$$\frac{1}{q_e} = \frac{1}{Q^0} + \frac{1}{bQ^0} \frac{1}{C_e} \quad (9)$$

Langmuir constants  $Q^0$  and  $b$  can be calculated from the linear plots of  $1/q_e$  versus  $1/C_e$  of slope and intercept respectively. It gives a straight line of slope  $1/bQ^0$  and intercepts  $1/Q^0$ . The theoretical maximum adsorption capacity  $Q^0$  corresponding to Langmuir constant is numerically equal to  $bQ^0$ . The constant  $b$  represents affinity between adsorbent and sorbate.

Freundlich isotherm is the earliest known relationship describing the sorption equation. This fairly satisfactory empirical isotherm can be used for non-ideal sorption that involves heterogeneous sorption and is expressed by the following equation:

$$q_e = K_f C_e^n \quad (10)$$

Where  $K_f$  and  $n$  are the Freundlich constants,  $K_f$  relates to sorption capacity and 'n' as sorption intensity. The logarithmic form of Equation (10) given below is usually used to fit data from the batch equilibrium studies.

$$\log q_e = \log K_f + \frac{1}{n} \log C_e \quad (11)$$

$K_f$  and 'n' can be calculated from the intercept  $\log K_f$  and slope  $1/n$  by plotting  $\log q_e$  versus  $C_e$ . It shows that the 'n' values of Freundlich model were  $1 < n < 3$  suggesting that adsorption of dye was favourable.

### 3. Results and discussions

#### 3.1. Photocatalytic degradation of Procion blue H-B dye

##### 3.1.1. Effect of flow rate

Degradation studies were conducted with different flow rates of 20, 40, 60, 80 and 100 mL/min. Figure 3 shows the effect of flow rates on colour removal. From this figure it was clear that, degradation rate gradually decreased with the increases of flow rate. It is due to the fact that increase of flow rate also increases the thickness of washwater which flows inside the walls of the

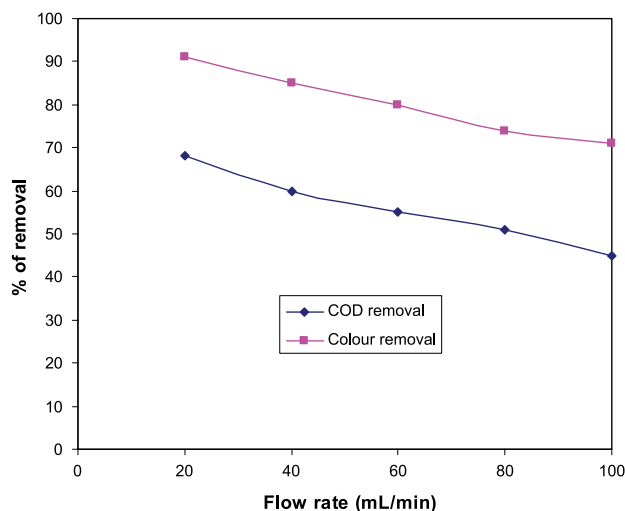


Figure 3. Effect of flow rate.

reactor. Matthews [24] has reported that, an increase in the flow rate through an illuminated spiral increases the photocatalytic oxidation rate of several solutes. Based on the experimental results the maximum degradation and colour removal have occurred at the minimum flow rate of 20 mL/min for both catalysts because of the greater residence time.

##### 3.1.2. Effect of pH

Solution pH is an important variable in the evaluation of aqueous-phase-mediated photocatalytic reactions. It influences the adsorption and dissociation of the substrate, the catalyst surface charge, oxidation potential of the valence band and other physicochemical properties of the system [25,26,27]. The role of pH on the rate of photocatalytic degradation was studied by three different initial pH values of the washwater such as 3, 7 and 10. Figure 4 shows the effect of pH on the removal of colour and COD. From this figure, it was observed that the degradation decreased with an increase of pH, exhibiting maximum degradation rate at pH 3. At higher pH values the degradation rate decreased exponentially. The effect of pH can be explained on the basis of zero point charge [11] (pHzpc) of catalysts, the pH at which the concentrations of protonated and deprotonated surface groups are equal. At high solution pH (>3) there will be a higher concentration of dye anions. Since the dye has a sulphonic acid group in its structure, which is negatively charged, the acidic solution favours adsorption of dye onto the photocatalyst surface, thus the photodegradation efficiency increases. However, adsorption on the catalyst surface is hindered due to the negatively charged surface prevalent at pH values beyond the zero point charge of catalysts. At high pH, OH species will

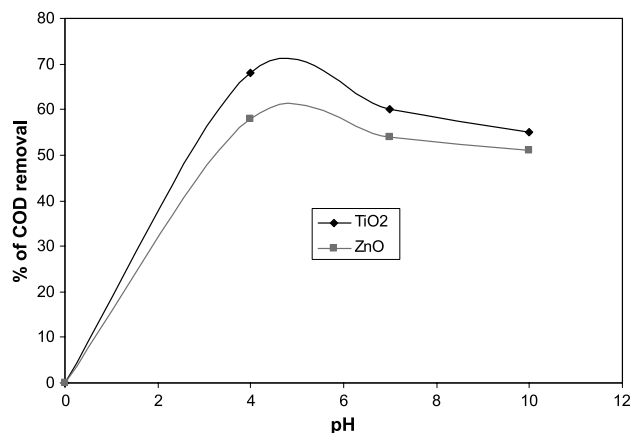


Figure 4. Effect of pH.

compete with dye anions for the available photo generated holes on the catalyst's surface.

### 3.1.3. Effect of initial concentration

During the dyeing process, the dyes fix on to the fibre in a way that depends on contact time, temperature, salinity and the dye's characteristic adsorption isotherm. It being impossible to determine the concentration of dye in the exhausted wastewater, the results obtained in this research were based on colour removal instead of dye concentration. The effect of initial concentration on decolorization efficiency has been investigated by varying the initial concentration of wastewater such as 20, 40, 60, 80 and 100 mg/L in the presence of TiO<sub>2</sub> and ZnO suspension, since the pollutant concentration is an important parameter in wastewater treatment. Experimental results are presented in Figure 5. It can be seen from the figure that the concentration has a significant effect on the degradation rates and rate of decrease in the dye concentration is faster

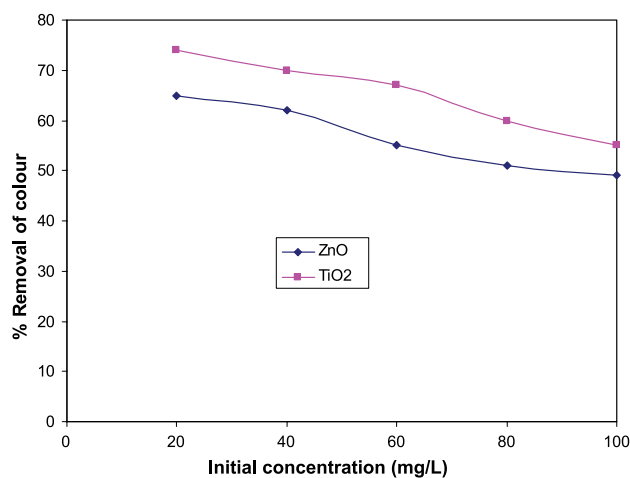


Figure 5. Effect of initial concentration.

when the initial concentration is less. The degradation rate is lower for higher initial concentration as the order decreases and, therefore, the Langmuir and Freundlich rate form was proposed to model the experimental data. The inset of the figure shows that initial rate increases with increase in initial concentrations and saturates at higher concentrations. The external diffusion is negligible in the concentration range of our investigation. Adsorption and surface reaction were assumed to be the rate controlling steps and these parameters were determined using Langmuir and Freundlich rate form. From the results it was observed that, in acidic solution (pH 3) maximum colour removal was 74% and 65% for TiO<sub>2</sub> and ZnO, respectively. The decolorization and degradation efficiencies are inversely related to the wastewater concentration. By increasing the concentration, the equilibrium adsorption of dye on catalyst surface sites increases, and as a result OH<sup>•</sup> radical formation rate decreases due to the hindered OH<sup>-</sup> ion adsorption at the same sites. In addition to that the path lengths of photons entering the solution also decrease according to the Beer Lambert law, which causes lower photonic absorption on catalyst particles and hence the photocatalytic reaction rate decreases.

### 3.1.4. Effect of catalyst loading

To investigate the effect of catalyst loading on decolorization efficiency, two sets of experiments were conducted employing TiO<sub>2</sub> and ZnO photo catalysts. The varying amounts of catalysts ranging from 100 to 500 mg/L were used. The result obtained, shown in Figure 6(a) and (b), suggests that both the catalysts showed the same trend, i.e., decolorization efficiency increased with increasing catalyst loading until a plateau was reached at a concentration of 300 and 400 mg/L respectively for TiO<sub>2</sub> and ZnO. This is because catalyst loading exhibits conflicting effects on the photocatalytic process; at lower loading levels, photonic adsorption controls the reaction extent due to the limited catalyst surface area, while at higher loading levels, light scattering by catalyst particles predominates over photonic adsorption [28,29]. Figure 7(a) and (b) shows the degradation of wastewater on percentage removal of COD and colour. From the results, it was observed that, the maximum COD reduction efficiency was 68% for TiO<sub>2</sub> and 58% for ZnO. On the other hand, the colour removal efficiency was found to be 74% and 69%, respectively, for TiO<sub>2</sub>- and ZnO-assisted systems under optimum conditions.

### 3.1.5. Decolorization kinetics

A study of the adsorption kinetic is desirable because it provides information regarding the mechanism of

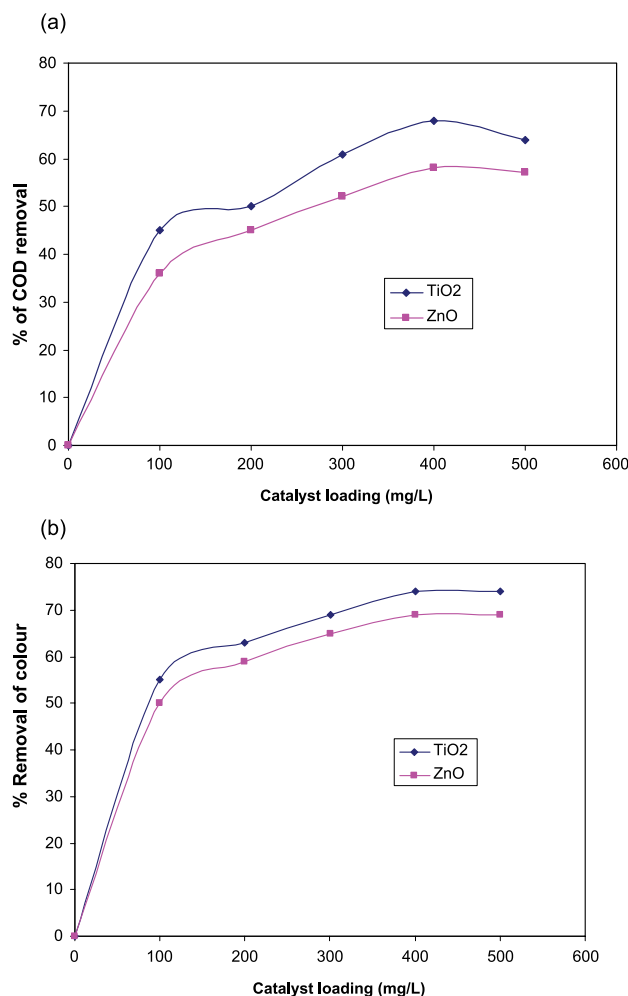


Figure 6. Effect of catalyst loading.

adsorption, which is important for the efficiency of the process. The experimental kinetic data of adsorption studies were applied to the first-order, second-order and intraparticle diffusion kinetic models and shown in the table 1(a) & (b). The correlation coefficients for the first-order kinetic model obtained at all the studied concentrations for ZnO were shown in Table 1(a), and the values of correlation coefficients were greater than 0.9 and the theoretical  $q_e$  values also agreed very well. This suggests that the pseudo first-order kinetic model was applicable when using Zinc oxide for the adsorption of Procion blue dye at lower and higher dye concentrations. The results indicate that correlation coefficient for second order is lower than that of first order for all dye concentrations and sorbent dosages. It was concluded that the second order kinetic model did not show a good correlation coefficient for adsorption of Procion blue dye. The correlation coefficients were always  $R^2 < 0.900$  also shown in Table 1(a). These results also show that the

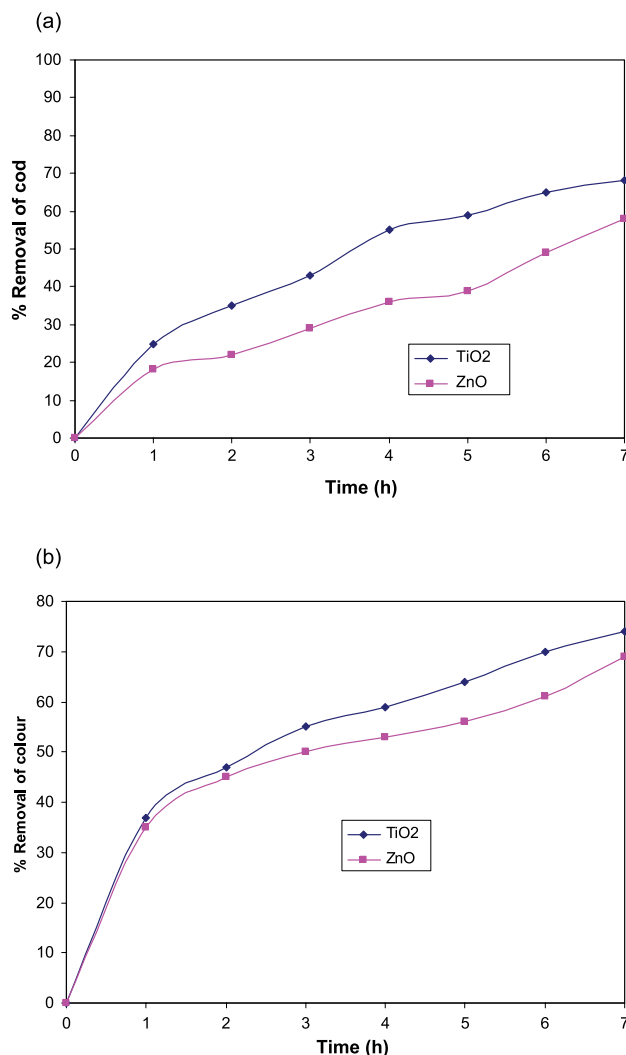


Figure 7. Photocatalytic degradation of Procion blue H-B dye on (a) COD removal (b) colour removal.

sorption system is not second-order reaction and it was the pseudo first-order. The intraparticle-diffusion kinetic model based on the assumption that the rate limiting step may be physical and chemical adsorption involving sharing or exchange of electron between dye anion and adsorbent, provides the best correlation of the data for the Procion blue dye onto Zinc oxide.

The rate constants and correlation coefficients for the adsorption of process blue dye molecules into titanium dioxide were presented in Table 1(b). The coefficient of correlation ( $R_2$ ) obtained by the pseudo first-order (mostly greater than 0.95), intraparticle-diffusion (mostly greater than 0.97) and the second-order kinetic model (not well described) suggests that the pseudo first-order and intraparticle-diffusion models are suitable for description of adsorption kinetic for the



Table 1. Kinetic data for (a) ZnO; (b) TiO<sub>2</sub>.

Table 1(a)

Dosage of ZnO (g)	Concentration of dye (mg/L)	Pseudo First-order			Second-order		Intraparticle-diffusion	
		K	q <sub>e</sub>	R <sub>1</sub> <sup>2</sup>	K <sub>2</sub>	R <sub>2</sub> <sup>2</sup>	K <sub>id</sub>	R <sub>3</sub> <sup>2</sup>
0.02	20	0.0077	147.4	0.97	—	0.92	7.08	0.98
	40	0.0089	272.7	0.95	—	0.95	13.37	0.98
	60	0.0088	395.4	0.96	—	0.91	19.37	0.98
	80	0.0081	502.1	0.96	—	0.93	23.99	0.97
	100	0.0082	570.4	0.96	—	0.63	27.12	0.97
0.04	20	0.0102	76.54	0.97	—	0.95	3.93	0.98
	40	0.0094	149.4	0.97	—	0.83	7.472	0.97
	60	0.0078	220.5	0.98	—	0.81	10.65	0.97
	80	0.0085	276.9	0.95	—	0.82	13.36	0.98
	100	0.0085	321.4	0.93	—	0.63	15.02	0.97
0.06	20	0.0102	53.7	0.96	—	0.93	2.73	0.98
	40	0.0095	102.2	0.96	—	0.87	5.08	0.98
	60	0.0077	136.6	0.97	—	0.90	6.58	0.98
	80	0.0079	167.2	0.95	0.001	0.92	7.97	0.98
	100	0.0067	200.9	0.96	—	0.21	9.05	0.97
0.08	20	0.0101	40.4	0.95	—	0.91	2.02	0.98
	40	0.0083	76.9	0.95	—	0.85	3.71	0.98
	60	0.0086	103.9	0.95	—	0.84	4.95	0.97
	80	0.0074	131.0	0.94	—	0.64	5.92	0.97
	100	0.0077	150.7	0.94	—	0.65	7.04	0.98
0.1	20	0.0077	33.1	0.94	—	0.84	1.66	0.97
	40	0.0079	63.2	0.96	—	0.82	2.97	0.97
	60	0.0081	88.3	0.95	0.002	0.96	4.20	0.98
	80	0.0072	114.4	0.96	—	0.91	5.27	0.97
	100	0.0080	135.1	0.95	—	0.61	6.24	0.97

Table 1(b)

S.NO	Dosage of TiO <sub>2</sub> (g)	Concentration of dye (mg/L)	Pseudo first-order			Second-order		Particle-diffusion	
			K	q <sub>e</sub>	R <sub>1</sub> <sup>2</sup>	K <sub>2</sub>	R <sub>2</sub> <sup>2</sup>	K <sub>id</sub>	R <sub>3</sub> <sup>2</sup>
1.	0.02	20	0.0082	132.2	0.98	—	0.98	6.6	0.98
		40	0.0084	242.4	0.95	—	0.93	11.5	0.98
		60	0.0078	337.2	0.93	—	—	15.2	0.97
		80	0.0073	390	0.93	—	—	17.1	0.96
		100	0.0076	416	0.95	—	—	18.6	0.96
2.	0.04	20	0.0087	71.2	0.99	0.002	0.99	3.8	0.97
		40	0.0096	129.6	0.99	—	0.98	6.9	0.98
		60	0.0084	186.8	0.99	—	0.99	9.6	0.98
		80	0.0099	225.7	0.96	—	0.97	11.7	0.98
		100	0.0088	253.6	0.98	—	—	12.7	0.97
3.	0.06	20	0.0095	49.7	0.97	—	—	2.4	0.96
		40	0.0108	90.9	0.96	—	—	4.4	0.96
		60	0.0104	132.5	0.95	—	—	6.3	0.95
		80	0.0098	167.7	0.95	—	—	7.8	0.95
		100	0.0085	204.7	0.95	—	—	9.2	0.94

Table 1. (Continued).

Table 1(b)									
S.NO	Dosage of TiO <sub>2</sub> (g)	Concentration of dye (mg/L)	Pseudo first-order			Second-order		Particle-diffusion	
			K	q <sub>e</sub>	R <sub>1</sub> <sup>2</sup>	K <sub>2</sub>	R <sub>2</sub> <sup>2</sup>	K <sub>id</sub>	R <sub>3</sub> <sup>2</sup>
4.	0.08	20	0.0096	38.6	0.99	0.001	0.96	2.0	0.98
		40	0.0089	73.0	0.98	—	0.87	3.7	0.97
		60	0.0081	105	0.97	—	—	3.7	0.97
		80	0.0078	133.8	0.97	—	—	6.2	0.97
		100	0.0080	158.1	0.94	—	—	7.3	0.96
5.	0.1	20	0.0098	31.3	0.97	0.002	0.97	1.6	0.98
		40	0.0100	59.6	0.94	—	0.97	3.0	0.98
		60	0.0095	84.6	0.96	—	0.94	4.3	0.98
		80	0.0089	107.7	0.96	—	0.83	5.3	0.98
		100	0.0092	128.5	0.95	—	—	6.3	0.97

Table 2. Values of isotherm constants (a) ZnO; (b) TiO<sub>2</sub>.

Table 2(a)								
Dosage of ZnO (g)	Linear		Langmuir		Freundlich			
	K <sub>D</sub>	R <sub>2</sub> <sup>2</sup>	Q <sup>0</sup>	b	RL <sub>2</sub> <sup>2</sup>	K <sub>f</sub>	n	RF <sub>2</sub> <sup>2</sup>
0.02	11.29	0.97	632.9	0.03	0.998	5.48	1.50	0.99
0.04	7.73	0.96	380.2	0.02	0.999	4.19	1.39	0.99
0.06	3.81	0.98	315.4	0.06	0.998	4.20	1.83	0.99
0.08	2.96	0.97	261.0	0.06	0.999	3.69	1.79	0.99
0.1	3.46	0.98	205.7	2.44	0.998	3.32	1.59	0.99

Table 2(b)								
Dosage of TiO <sub>2</sub> (g)	Linear		Langmuir		Freundlich			
	K <sub>D</sub>	R <sub>2</sub> <sup>2</sup>	Q <sup>0</sup>	b	RL <sub>2</sub> <sup>2</sup>	K <sub>f</sub>	n	RF <sub>2</sub> <sup>2</sup>
0.02	5.26	0.92	47.3	0.039	0.99	5.5	1.83	0.97
0.04	4.12	0.96	21.4	0.039	0.99	4.1	1.64	0.99
0.06	4.58	0.99	15.5	0.036	0.99	3.2	1.42	0.99
0.08	3.68	0.98	15.9	0.037	0.99	3.1	1.46	0.99
0.1	3.03	0.98	8.56	0.041	0.99	2.9	1.49	0.99

removal of dye from aqueous solution into titanium dioxide. The second-order kinetic model was not suitable to describe the adsorption of Procion blue dye.

### 3.1.6. Adsorption effects of TiO<sub>2</sub> and ZnO

The analysis of isotherm data is important to develop the equations that represent the results and would be useful to design degradation purpose [30]. For heterogeneous photo catalysis adsorption on catalyst surface is a

prerequisite condition [31]. It has been observed that the amount of adsorption per gram of adsorbate increases with the rise of concentration. In this study two isotherms namely, Langmuir and Freundlich isotherms have been selected to evaluate the adsorption capacity of the adsorbents (TiO<sub>2</sub> and ZnO). The values of isotherm constants with the correlation coefficients were listed in Table 2(a) and (b). This shows the high values of correlation coefficients R<sub>L</sub><sup>2</sup> and R<sub>F</sub><sup>2</sup> which indicate that both the Langmuir and Freundlich isotherms fit well. From the Table, it was also evident

that  $Q^0$  values of Zinc oxide were more than those of Titanium dioxide. It shows that the amount of adsorption per gram of adsorbate was more. Also the initial concentration of dye gives the maximum adsorption of dye at free sites of the surface of particles of catalyst and hence all sites are occupied. This concentration adsorbed becomes constant and there is formation of a monolayer and heterogeneous [32].

#### 4. Conclusion

The photocatalytic degradation of a pollutant Procion blue H-B dye in textile washwater was studied using two photo catalysts TiO and ZnO. For the chosen pollutant, Procion blue H-B dye, two methods of oxidation were observed. Oxidation with OH<sup>•</sup> radicals originating on the surface of the photocatalyst; direct oxidation by holes created by the action of light on the semiconductor. Nevertheless, after a long irradiation time (7 hrs), the maximum COD reduction efficiency was 68% for TiO<sub>2</sub> and 58% for ZnO. On the other hand, the colour removal efficiency was found to be 91% and 82%, respectively for TiO<sub>2</sub>- and ZnO-assisted systems under optimum conditions. The data obtained is well fitted with Freundlich and Langmuir adsorption isotherms. Under all experimental conditions TiO<sub>2</sub> showed better catalytic properties over ZnO subject to both adsorption and decolorization. Under the experimental condition described, it was noticed that decolorization mechanism of Procion blue dye follows pseudo first order kinetics over TiO<sub>2</sub>/ZnO surfaces.

#### Acknowledgement

The authors wish to thank the Director, Central Electrochemical Research Institute, Karaikudi for the kind encouragement given.

#### References

- [1] C. O'Neill, F.R. Hawkes, D.L. Hawkes, N.D. Lourenço, H.M. Pinheiro, and W. Delee, *Color in textile effluents—sources, measurement, discharge consents and simulation: a review*, J. Chem. Technol. Biotechnology. 74 (1999), pp. 1009–1018.
- [2] A.M. Talarposhti, T. Donnelly, and G.K. Anderson, *Color removal from a simulated dye wastewater using a two-phase anaerobic packed bed reactor*, Water Res. 35 (2001), pp. 425–432.
- [3] H. Feitkenhauer and U. Meyer, *The integration of an anaerobic wastewater pretreatment in the water management concept of a plant*, Melland Textiles 80 (1999), pp. E82–E84.
- [4] J.S. Chang, C. Chou, and S.Y. Chen, *Decolorization of azo dyes with immobilized Pseudomonas Luteola*, Process Biochem. 36 (2001), pp. 757–763.
- [5] O.J. Hao, H. Kim and P.C. Chiang, *Decolorization of wastewater*, Critical Reviews in Environ. Sci. Technol. 30 (2000), pp. 449–505.
- [6] P.C. Vandevivere, R. Bianchi, and W. Verstraete, *Treatment and reuse of wastewater from textile wet-processing industry: review of emerging technologies*, J. Chem. Technol. Biotechnology. 72 (1998), pp. 89–302.
- [7] V. Oles, W. Hellmann, and D. Lazar, *The costs of effluent treatment in the textile finishing industry*, Melland Textiles 76 (1995), pp. E182–E184.
- [8] E.V. Hess, *Environmental chemicals and autoimmune disease: cause and effect*, Toxicology, 181–182 (2002), pp. 65–70.
- [9] I. Poullos D. Makri, and X. Prohaska, *Photocatalytic treatment of olive milling waste water: oxidation of protocatechuic acid*, GNEST. Int. Journal 1 (1999), pp. 55–62.
- [10] U. Pagga and D. Brown, *The degradation of dyestuffs: Part II Behaviour of dyestuffs in aerobic biodegradation tests*, Chemosphere 15 (1986), pp. 479–491.
- [11] K.H. Gregor, *Oxidative decolorization of textile waste water with advanced oxidation processes*. In *Chemical Oxidation, Technologies for the Nineties*, W. Eckenfelder, A. Bowers, and J. Roth, eds., Lancaster- Basel, 1994, pp. 161–193.
- [12] W.G. Kuo, *Decolorizing dye wastewater with Fenton's reagent*, Water Res. 26 (1992), pp. 881–886.
- [13] T. Watanabe, K. Hashimoto, and A. Fujishima, in *Photocatalytic Purification and Treatment of Water and Air*, D.F. Ollis, and H. Al-Ekabi, eds., Elsevier, Amsterdam, 1993, p. 139.
- [14] M.A. Fox and M. T. Dually, *Heterogeneous photo catalysis*, Chem. Rev. 93 (1993), pp. 341–357.
- [15] P.V. Kamat, *Photochemistry on nonreactive and reactive (semiconductor) surfaces*, Chem. Rev. 93 (1993), pp. 26–300.
- [16] D.W. Bahnemann, D. Bockelmann, R. Goslich, and M. Hilgendorff, *Photocatalytic detoxification of polluted aquifers: novel catalysts and solar applications*, In *Aquatic and Surface Photochemistry* G.R. Helz, R.G. Zepp, and D.G. Crosby, eds., Lewis – CRC Press, Boca Raton, 1994, pp. 154–167.
- [17] V. Laszlo, J. Terence, and J. Kemp, *Light flux and light flux density dependence of the photo mineralization rate of 2, 4-dichlorophenol and chloroacetic acid in the presence of TiO<sub>2</sub>*, Photochem. Photobiol. 87 (1995), pp. 25–260.
- [18] W.H. Glaze, J.F. Kennebec, and J.L. Ferry, *Chlorinated byproducts from the titanium oxide-mediated photodegradation of trichloroethylene and tetrachloroethylene in water*, Environ. Sci. Technol. 27 (1993), pp. 177–184.
- [19] D. Ollis, E. Pelizzetti, and N. Serpone, *Heterogeneous photo catalysis in the environment: application to water purification*. In *Photo catalysis: Fundamentals and Applications*, N. Serpone, E. Pelizzetti, eds., John Wiley & Sons, New York, 1989, pp. 603–637.
- [20] M.R. Hoffmann, S.T. Martin, W. Choi, and D.W. Bahnemann, *Environmental Applications of Semiconductor Photo catalysis*, Chem. Rev. 95 (1995), pp. 69–96.
- [21] C. Namasivayam and K. Ranganathan, *Recycling of 'waste' Fe (III)/Cr (III) hydroxide for the removal of nickel from wastewater: adsorption and equilibrium studies*, Waste Manage. 14 (1994), pp. 709–716.
- [22] G. McKay and Y.S. Ho, *The sorption of lead (II) ions on peat*, Water Res. 33 (1999), pp. 578–584.
- [23] W.J. Weber and C.J. Morris, *Proc. First Int. Conf. Wat. Poll. Res.* 2 (1962), p. 231.

- [24] R.W. Matthews, *Photooxidation of organic impurities in water using thin films of titanium dioxide*, J. Phys Chem., 91 (1987), pp. 3328–3333.
- [25] L. Gebrati, L. Loukili Idrissi, Y. Mountassir, and A. Nejmeddine, Detoxification of textile industry effluents by photocatalytic treatment, Environ Technol. 31 (2010), pp. 625–632.
- [26] S. Sakthivel, M.V. Shankar, M. Palanichamy, B. Arabin-doo and V. Murugesan, *Photocatalytic decomposition of leather dye: comparative study of  $\text{TiO}_2$  supported on alumina and glass beads*, J. Photochem Photobiol. 148 (2002), pp. 153–159.
- [27] A. Rezaee, M.T. Ghaneian, N. Taghavinia, M.K. Aminian, and S.J. Hashemian,  *$\text{TiO}_2$  nanofibre assisted photocatalytic degradation of Reactive Blue 19 dye from aqueous solution*, Environ Technol. 30 (2009), pp. 233–239.
- [28] A. Akyol, H.C. Yatmaz, and M. Bayramoglu, *Photocatalytic degradation of Remazol Red RR in aqueous ZnO suspension*, Appl. Catal. B. 54 (2004), pp. 19–24.
- [29] F. Kiriakidou D.I. Kondarides, and X.E. Verykios, *The effect of operational parameters and  $\text{TiO}_2$ -doping on the photocatalytic degradation of azo-dyes*, Catal. Today, 54 (1999), pp. 119–30.
- [30] C. Namasivayam, R. Jeyakumar, and R.T. Yamuna, *Dye removal from wastewater by adsorption on 'waste' Fe (III)/Cr (III) hydroxide*, Waste Manage. 14 (1994), pp. 643–648.
- [31] M.A. Hasnat, I.A. Siddiquey, and S.M. Saiful, *Photodegradation of malachite green in the aqueous medium*, Indian J. Chem. A 4 (2003), pp. 1865–1867.
- [32] A.R. Khataee, *Photocatalytic removal of C.I. Basic Red 46 on immobilized  $\text{TiO}_2$  nanoparticles: Artificial neural network modeling*, Environ Technol. 30 (2009), pp. 1155–1168.